Electronic Supplementary Information

Ni$_2$O$_3$-Au$^+$ Hybrid Active-Sites on NiO$_x$@Au Ensembles for Low-Temperature Gas-phase Oxidation of Alcohols

Guofeng Zhao [a], Huanyun Hu [a], Wei Chen [a], Zheng Jiang [b], Shuo Zhang [b], Jun Huang [*,c], Yong Lu [*, a]

([a] Shanghai Key Laboratory of Green Chemistry and Chemical Processes, Department of Chemistry, East China Normal University, 3663 North Zhongshan Road, Shanghai 200062, China

[b] Shanghai Synchrotron Radiation Facility, Shanghai Institute of Applied Physics, Chinese Academy of Sciences, Shanghai 201204, China

[c] School of Chemical and Biomolecular Engineering, University of Sydney, NSW 2006, Australia)

Fax: (+86)21-62233424, Email: _ylu@chem.ecnu.edu.cn_; _jun.huang@sydney.edu.au_)

Materials and Methods

Catalyst preparation

Sinter-locked three-dimensional microfibrous networks consisting of 5 vol% 8-μm Ni-fibers (or 8-μm Ti-fibers) and 95 vol% void volume were built using regular papermaking/sintering processes.[S1-S6] The Ni-fiber was manufactured by Western Metal Material Co., Ltd., Xi'an, China, and Ti-fiber (8 μm dia.) was purchased from IntraMicron, Ltd. (USA). Five grams of Ni-fiber (or Ti-fibers) chops (2-3 mm length) and 1.5 g of cellulose fibers were added to water (1 L) and vigorously stirred to produce a uniform suspension. The resulting suspension was transferred into the head box of a 159 mm diameter circular sheet former (ZCX-159A, Changchun, China), and a 159 mm circular preform was then formed by draining and drying in air. The preform paper was oxidized in air at 500 °C to remove the cellulosic binders and subsequently sintered in hydrogen at 950 °C to create the three-dimensional sinter-locked networks.

NiO$_x$@Au/Ni-fiber: Gold was first galvanically deposited on this sinter-locked Ni-fiber (Ni + HAuCl$_4$ → Au + NiCl$_2$, $\varphi(Au^{3+}/Au^0) - \varphi(Ni^{2+}/Ni^0) = 1.5 - (-0.25) = 1.75$ eV) by incipiently impregnating it with an aqueous solution containing the specified amount of HAuCl$_4$ at room temperature. The resulting sample were dried overnight at 80 °C and calcined in air at 300 °C for 2 h to obtain the fresh Au/Ni-fiber catalyst. Then, the catalyst was pre-activated over the gas-phase oxidation of benzyl alcohol at 380 °C for 1 h using the molar ratio of O$_2$ to alcoholic hydroxyl molar ratio (O$_2$/hydroxyl) = 0.6 and weight hourly space velocity (WHSV) = 20 h^{-1}. During the pre-activated process, the NiCl$_2$ was transformed into NiO$_x$ (NiO$_x$ (assuming all is NiO) loading is calculated to be 2.4 wt% according to the galvanic reaction between Ni-fiber and HAuCl$_4$), which partially cover the gold particles to form the active

$NiO_x@Au$ ensembles. Finally, the pre-activated catalyst $NiO_x@Au$/Ni-fiber was obtained.

Au/Ni-fiber-W, Au/Ti-fiber and Au/NiO-Ni-fiber: These model catalysts were prepared by incipiently impregnating the corresponding sintered-fibers with aqueous solution containing appointed amount of $HAuCl_4$ at room temperature. The catalyst Au/Ni-fiber-W was obtained by washing the as-prepared catalyst Au/Ni-fiber using deionized water to remove the produced $NiCl_2$ (from the reaction: $HAuCl_4 + Ni \rightarrow Au + NiCl_2$) just after galvanic reaction and before drying. The catalyst Au/NiO-Ni-fiber was prepared using the Ni-fibers (calcined at 600 ^{o}C in air for 2 h). All the resulting samples were dried at 80 ^{o}C overnight and calcined at 300 ^{o}C for 2h in air and these samples were named as fresh samples.

NiO_x/Ni-fiber, $NiO_x@Au$/Ni-fiber-W, NiO_x/Ti-fiber, $NiO_x@Au$/Ti-fiber, $NiO_x@Au$/NiO-Ni-fiber: The five model catalysts were prepared by incipiently impregnating the corresponding sintered-fibers (Ni-fiber and Ti-fiber) and samples (Au/Ni-fiber-W, Au/Ti-fiber and Au/NiO-Ni-fiber) with aqueous solution containing appointed amount of $Ni(NO_3)_2$ (Sinopharm Chemical Reagent Co. Ltd, China) at room temperature. All the resulting samples were dried at 80 ^{o}C overnight and calcined at 300 ^{o}C for 2h in air and these samples were named as fresh samples.

The activated samples (or working samples) were obtained by pre-activating the fresh samples at 380 ^{o}C for 1h in reaction steam of benzyl alcohol (Sinopharm Chemical Reagent Co. Ltd, China) using the molar ratio of O_2 to alcoholic hydroxyl molar ratio (O_2/hydroxyl) = 0.6 and weight hourly space velocity (WHSV) = 20 h^{-1}.

Characterization

The X-ray powder diffraction (XRD) patterns were measured on a Rigaku Uitima IV diffractometer

with Cu Kα radiation at an acceleration voltage of 40 kV. The catalysts were also characterized by a transmission electron microscope (TEM, JEOL-JEM-2010 instrument at 200 kV). X-ray photoelectron spectra (XPS) were recorded on a VG EscaLab 220i spectrometer using a standard Al Kα X-ray source (300 W) and an analyzer pass energy of 20 eV. All binding energies were referenced to the adventitious C1s line at 284.9 eV. X-ray absorption fine structure (XAFS) data of the Ni K-edge (8,333 eV) and Au L^{III}-edge (11,919 eV) were collected in the transmission mode on the BL14W1 beamline of the Shanghai Synchrotron Radiation Facility (SSRF). The typical electron beam energy was 3.5 GeV, and the current was 300 mA. A cryogenically cooled double-crystal Si(111) monochromator was used to minimize the harmonics. The XAFS spectra were analyzed by the NSRLXAFS 3.0 package according to standard procedures.[S7] The experimental backscattering amplitude and phase shift for the Au-Au pair were extracted from the Au foil.

Gold loading of the typical NiO_x@Au/Ni-fiber was determined to be 3.8 wt% by inductively coupled plasma atomic emission spectrometry (ICP-AES) on a Thermo Scientific iCAP 6300 ICP spectrometer. As for the Ni-content, the support fiber is pure metal nickel. It should be noted that the NiO_x@Au ensembles rather than Au@Ni-fiber contributed to the low-temperature oxidation of alcohols. Therefore, the NiO_x-content of the NiO_x@Au ensembles can be the representative Ni-content of the catalyst. The NiOx-content can be estimated according to the galvanic reaction between Ni-fiber and $HAuCl_4$ ($3Ni + 2HAuCl_4 = 2HCl + 3NiCl_2 + 2Au$). The produced $NiCl_2$ was further transformed into NiO_x during the pre-activation period at 380 °C. Three moles of $NiCl_2/NiO_x$ were produced with the formation of two mole of Au. It indicates that 3.8 wt% of Au-content related to the $NiCl_2$ content of 4.2 wt% and the NiO_x (assuming all is NiO) content of 2.4 wt%.

Reactivity tests

The gas-phase selective oxidation of alcohols on these catalysts with molecular oxygen was performed on a fixed-bed quartz tube reactor (700 mm length by 16 mm inner diameter) under atmospheric pressure as described previously.[S5,S6,S8] Circular chips (16.1 mm diameter) of the microfibrous-structured catalysts were punched down from their large sheet sample and packed layer-up-layer into the tube reactor. The catalyst used in testing experiments is 0.3 g, corresponding to a bed thickness of 5 mm. Notice that the 0.1 mm larger diameter than the inner diameter of the tubular reactor was deliberately retained to avoid the appearance of a gap between the reactor wall and the edges of the catalyst chips, thereby preventing gas bypass. Alcohols were continuously fed with the speed of 6 g/h using a high-performance liquid pump in parallel with O_2 (oxidant of 13.6 ml/min) and N_2 (diluted gas of 100 ml/min) feeding using calibrated mass flow controllers into the reactor heated to the desired reaction temperature. WHSV was calculated by dividing the mass flow rate of alcohol feedstock by the catalyst mass. The effluent was cooled using an ice-salt bath (-15 ºC) to liquefy the condensable vapors for analysis using an HP 5890 gas chromatography-flame ionization detector (GC-FID) with a 60 m HP-5ms capillary column. The gas-phase products, such as H_2, CO_x, and C1-C3 hydrocarbons, were analyzed using an HP-5890 GC with thermal conductivity detector (TCD) and a 30 m AT-plot 300 capillary column.

Supplementary Figures and Tables
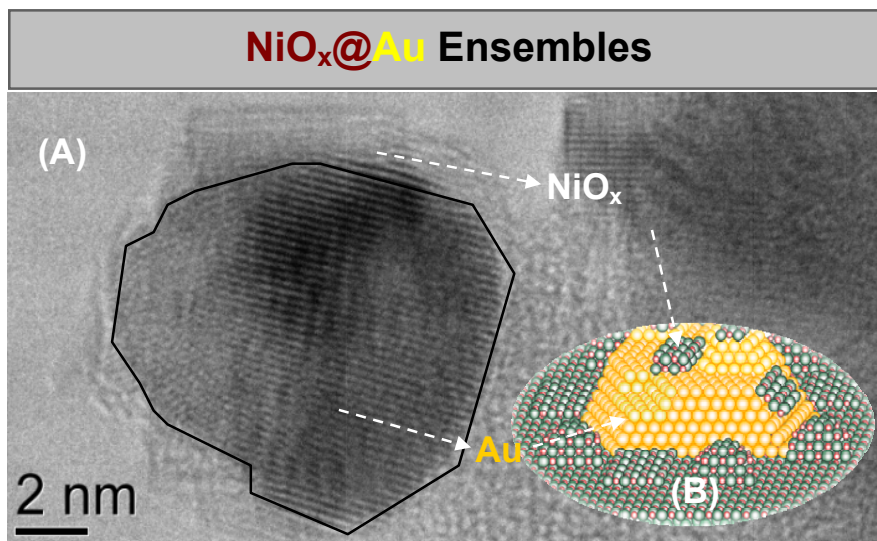
Fig. S1. Structure and model of the active $NiO_x@Au$ ensembles, with NiO_x segments partially covering large gold particles to form the ensembles. (A) TEM image of the active $NiO_x@Au$ ensembles over the pre-activated $NiO_x@Au$/Ni-fiber catalyst; (B) Structural illustration of the partial coverage of Au particles with NiO_x segments. Pre-activation conditions: undergoing benzyl alcohol oxidation at 380 ^{o}C for 1 h using O_2/ol = 0.6 and WHSV = 20 h^{-1}.
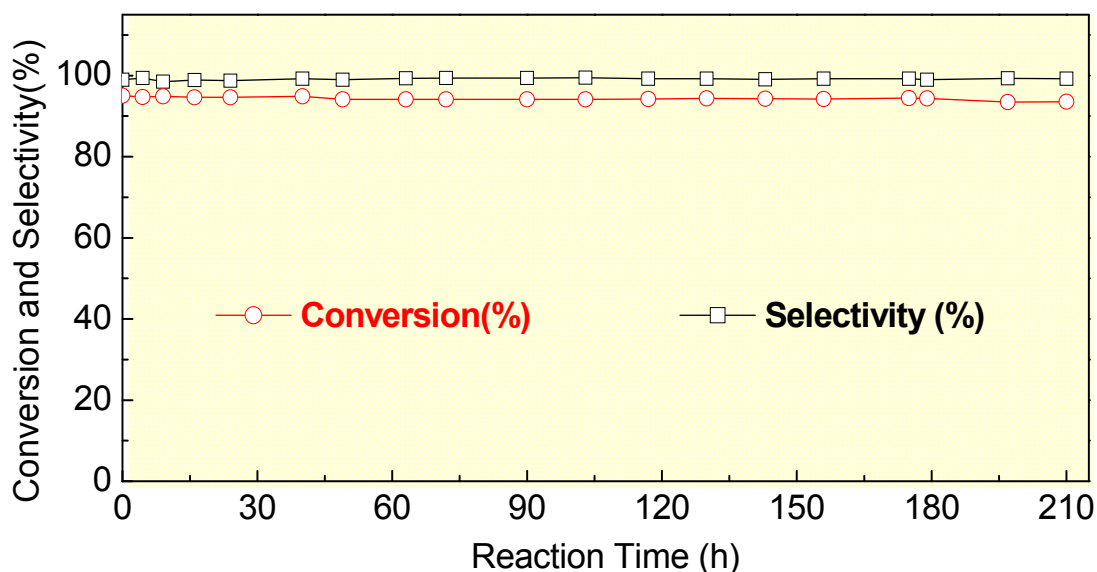
Fig. S2. Longer-term test over the pre-activated catalyst NiO_x@Au/Ni-fiber in the gas-phase oxidation of benzyl alcohol. Reaction conditions: 250 °C, O_2/hydroxyl = 0.6, WHSV = 20 h^{-1}. Pre-activation conditions: pre-activating the fresh samples at 380 °C for 1h in reaction steam of benzyl alcohol using O_2/hydroxyl = 0.6 and WHSV = 20 h^{-1}. ***Note***: In the whole process, 1.2 kg of benzyl alcohol was consumed. The average benzyl alcohol conversion and benzaldehyde selectivity is 93% and 99.2%, respectively, and the 0.8% selectivity is contributed to toluene (0.05%) and benzoic acid (0.75%). Therefore, the ideal and actual mass of the product based on the above conversion and selectivity is 1352.4 and 1350.2 g, respectively. Therefore, the mass balance is about 99.9%. In order to determine the experimental error of the conversion and selectivity, every product sample was analyzed by GC for 5 times, and the error is in the range of ±0.2%.
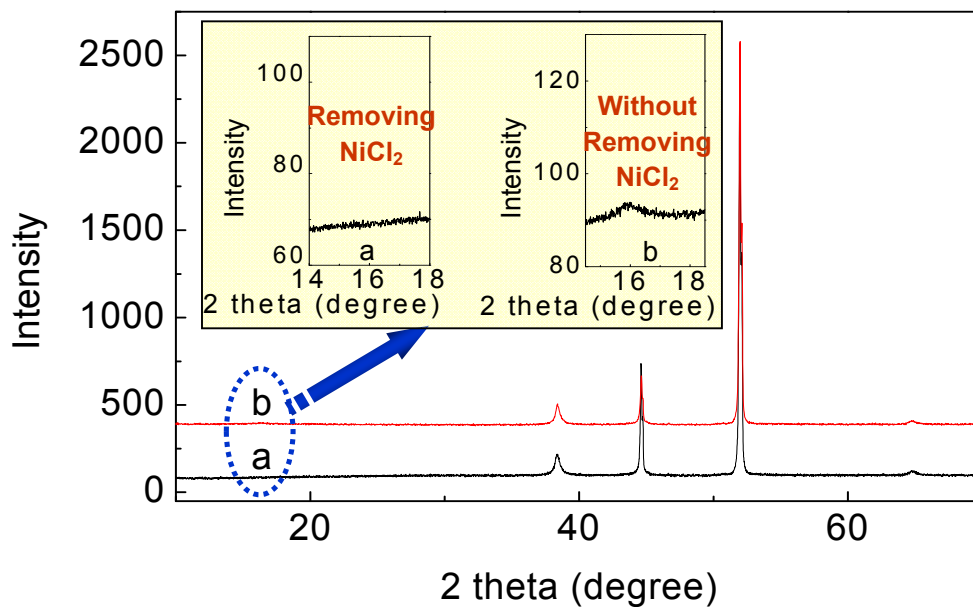
Fig. S3. XRD patterns of the Au/Ni-fiber catalysts (Au loading of 4 wt%) with $NiCl_2$ and without $NiCl_2$. (a) Removing $NiCl_2$ by washing the samples for 5 times using deionized water before drying and calcining (*i.e.*, just after galvanic exchange reaction); (b) Without removing $NiCl_2$. **Insert-a**: showing no $NiCl_2$ peak at $2\theta = 16^{\circ}$; **Insert-b**: showing the $NiCl_2$ peak at $2\theta = 16^{\circ}$.
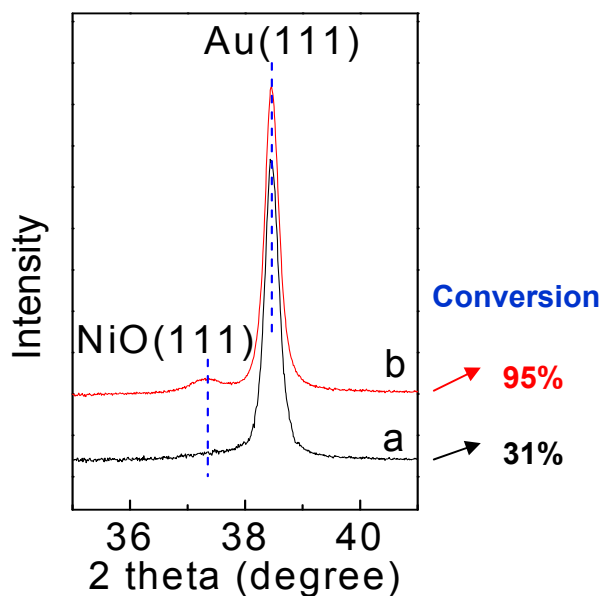
Fig. S4. XRD patterns of the pre-activated Au/Ni-fiber catalyst (Au loading of 4 wt%) with NiO_x and without NiO_x. (a) With the presence of NiO_x; (b) Removing NiO_x from the catalyst. Pre-activation and reaction conditions: the same as in Fig. S1.
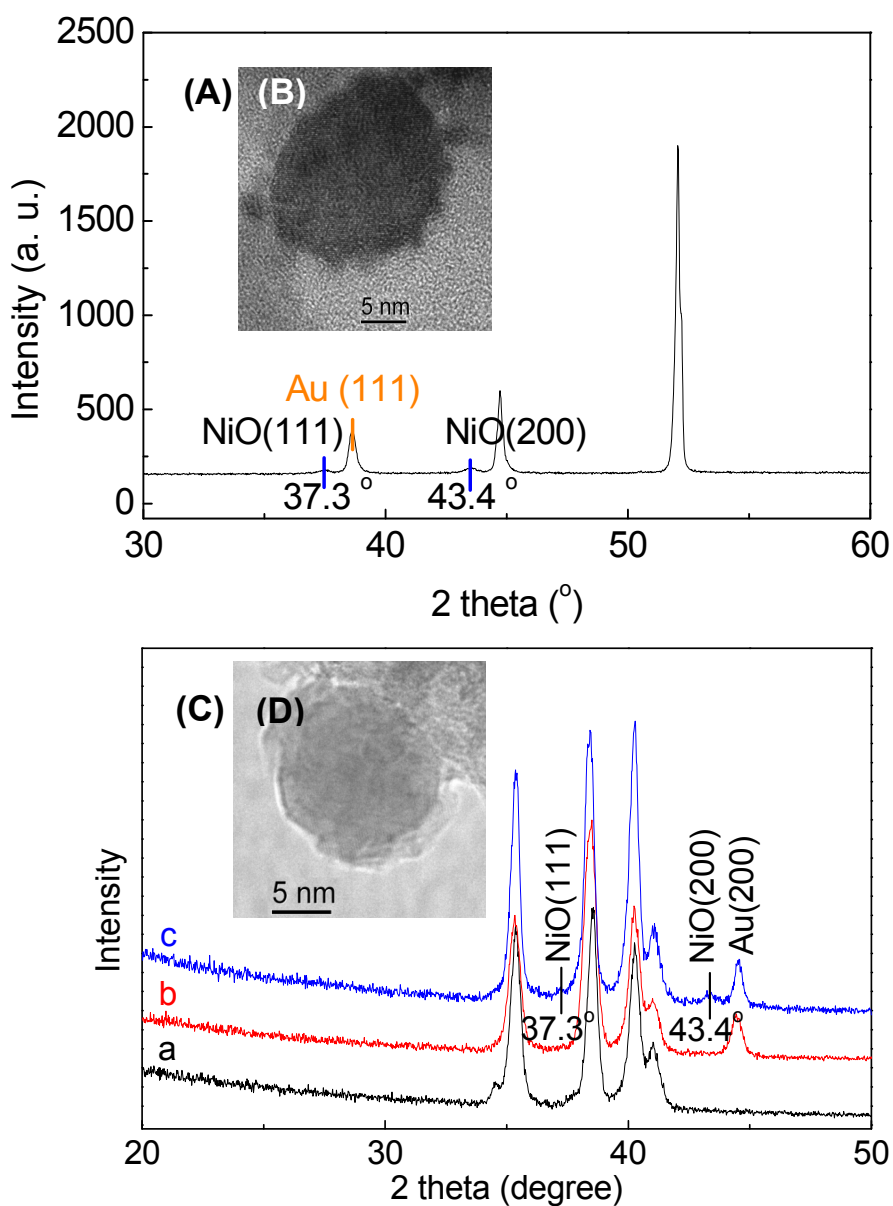
Fig. S5. The formation of the active NiO$_x$@Au ensembles over the catalysts NiO$_x$@Au/Ni-fiber-W and NiO$_x$@Au/Ti-fiber. XRD pattern (A) and TEM image (B) of the catalyst NiO$_x$@Au/Ni-fiber-W; XRD pattern (C) and TEM image (D) of the catalyst NiO$_x$@Au/Ti-fiber: (a) pure sinter-locked Ti-microfiber, (b) the pre-activated Au/Ti-fiber, and (c) the pre-activated NiO$_x$@Au/Ti-fiber. Pre-activation conditions: undergoing benzyl alcohol oxidation at 380 °C for 1 h using O$_2$/ol = 0.6 and WHSV = 20 h^{-1}.
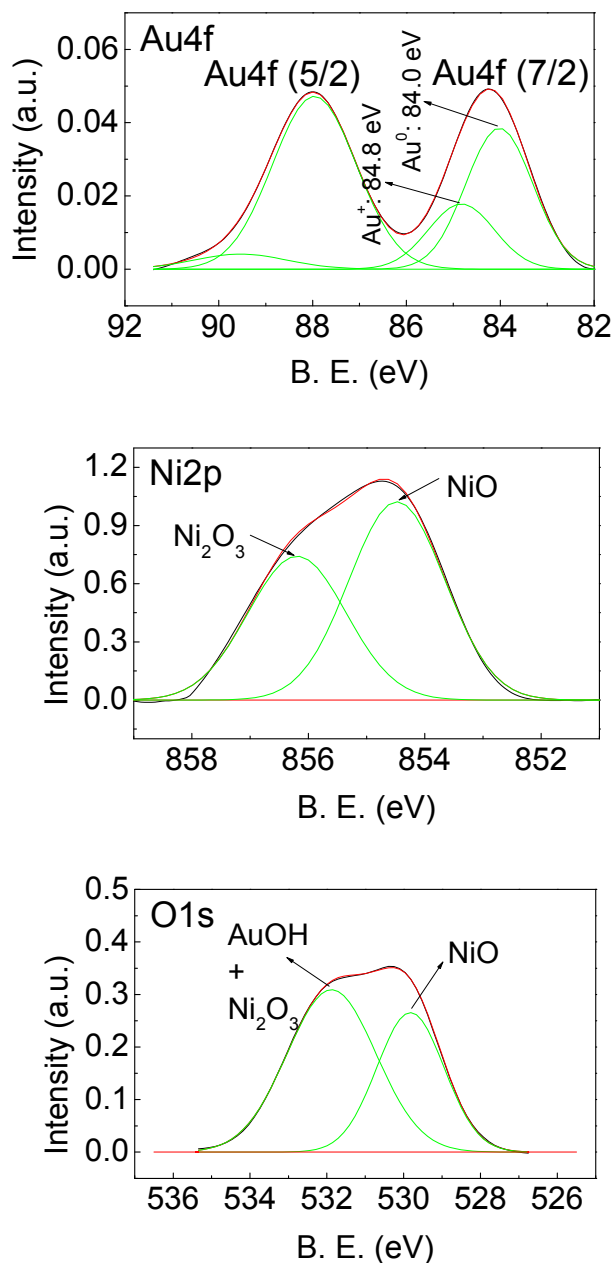
Fig. S6. XPS spectra in Au4f and Ni2p regions for the pre-activated NiO_x@Au/Ni-fiber catalyst. Coexistence of Au^0 together with Au^+, Ni^{2+} (NiO), and Ni^{3+} (Ni_2O_3) supports the partial coverage structure of the active NiO_x@Au ensembles.
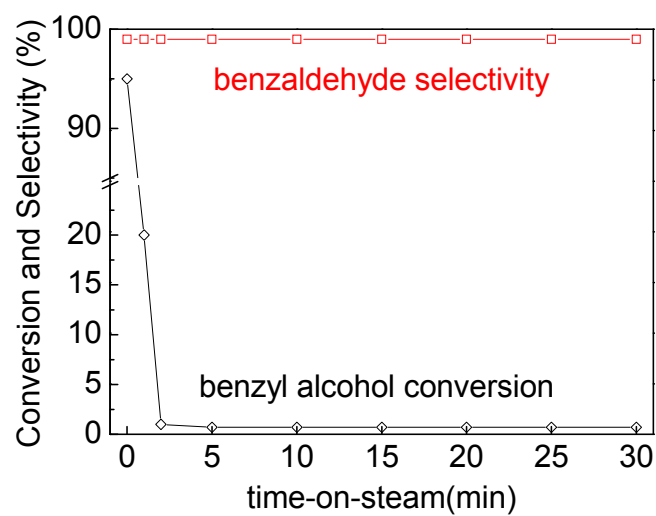
Fig. S7. The catalytic performance of the pre-activated NiO_x@Au/Ni-fiber over benzyl alcohol in the absence of O_2 at 250 ^{o}C with WHSV of 20 h^{-1}.
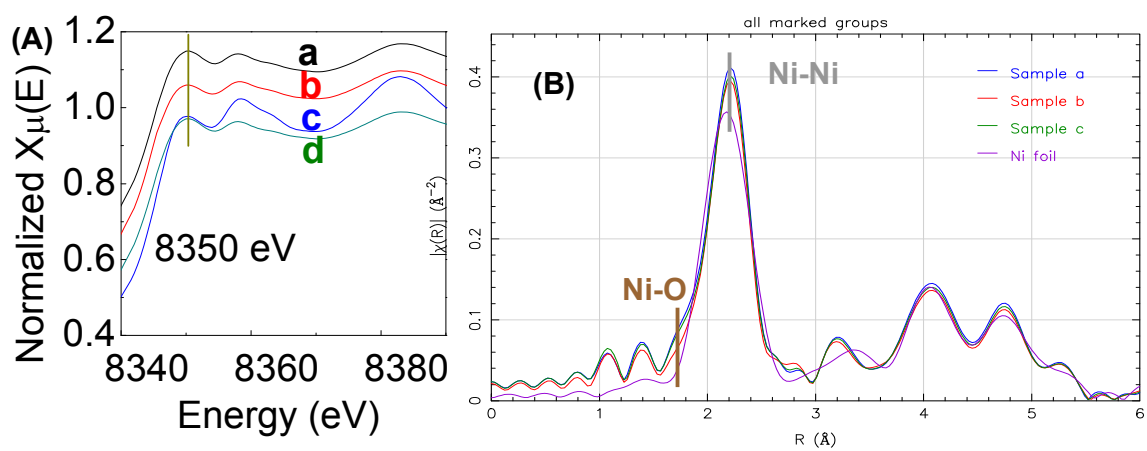
Fig. S8. Ni K-edge XANES (A) and modulus of the Fourier-transform (B) of Ni K edge signal. (a) The working catalyst NiO_x@Au/Ni-fiber; (b) The working sample after undergoing reaction with benzyl alcohol in the absence of O_2 at 250 °C for 0.5h (called exhaused catalyst); (c) Ni foil; (d) The exhausted catalyst catalyzing benzyl alcohol by re-feeding O_2 under the same conditions as in (a). Reaction conditions: same as in Fig. S1.
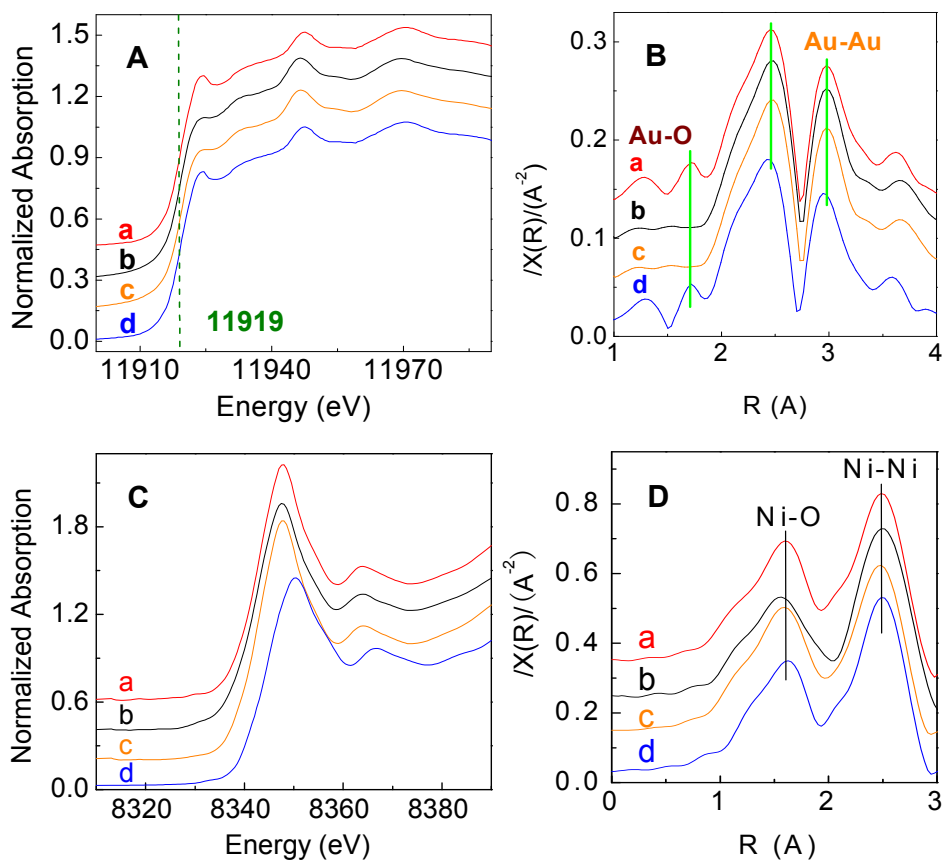
Fig. S9. XANES of Au L_3 edge (A) and modulus of the Fourier-transform of Au L_3 edge signal (B), and

XANES of Ni K-edge (C) and modulus of the Fourier-transform of Ni K edge signal (D) of several

catalysts. (A-B): (a) The working catalyst NiOx@Au/Ti-fiber after undergoing reaction with benzyl

alcohol in the presence of O_2 at 250 °C for 0.5h; (b) The working sample after undergoing reaction with

benzyl alcohol in the absence of O_2 at 250 °C for 0.5h (called exhausted catalyst); (c) Au foil; (d) The

exhausted catalyst catalyzing benzyl alcohol by re-feeding O_2 under the same conditions as in (a). (C-D):

(a) The same sample as in A-a; (b) The same sample as in A-b; (c) The same sample as in A-d; (d) Pure

NiO.
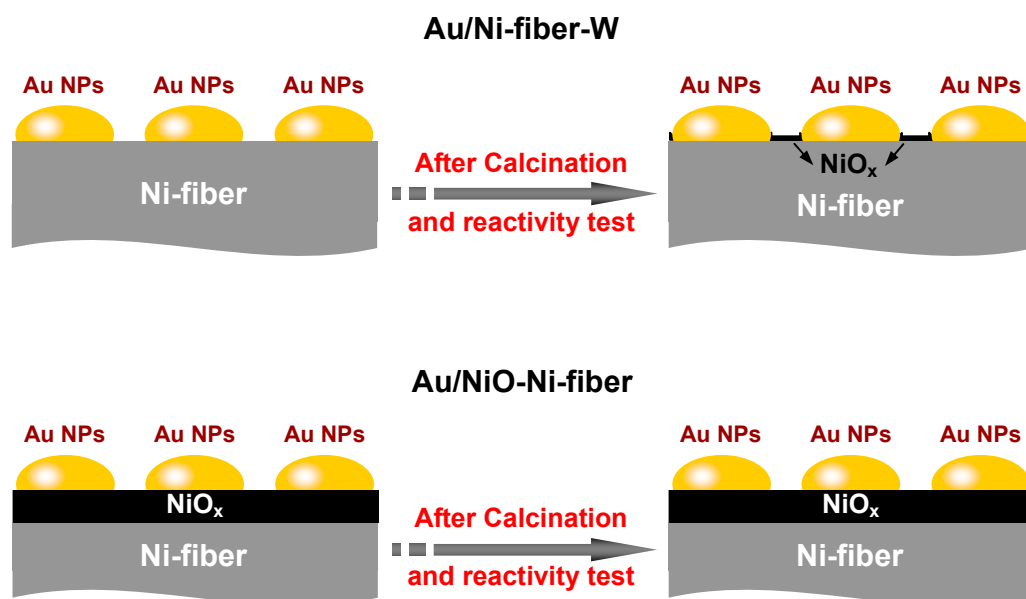
Scheme S1. Schematic illustration of the formation of a NiO_x circumference at the interface between Au-particles and fibrous support over the catalysts Au/Ni-fiber-W and Au/NiO-Ni-fiber (the same samples as in Table 1 (Entries 2 & 8, respectively) in manuscript) after calcination and reactivity test. The catalysts were pre-activated by undergoing the gas-phase oxidation of benzyl alcohol at 380 ^{o}C for 1 h using O_2/hydroxyl = 0.6 and WHSV = 20 h^{-1}, and then were tested at 250 ^{o}C using O_2/hydroxyl = 0.6 and WHSV = 20 h^{-1}.
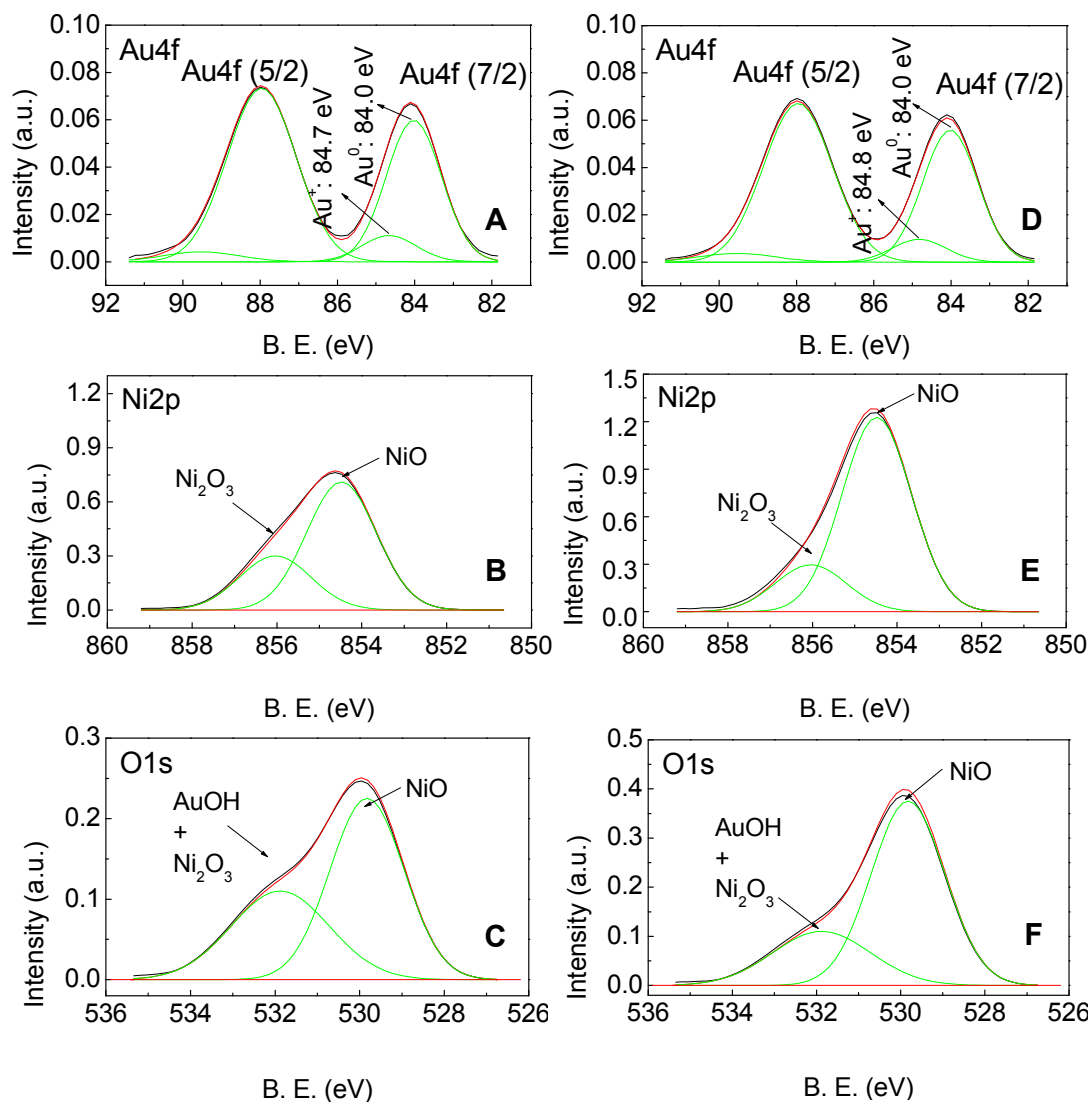
Fig. S10. XPS spectra in Au4f (A,D), Ni2p (B,E), and O1s (C,F) regions for the Au/Ni-fiber-W (A-C) and Au/NiO-Ni-fiber (D-F) catalysts (the same samples as in Table 1 (Entries 2 & 8, respectively) in manuscript) after reactivity test. The catalysts were pre-activated by undergoing the gas-phase oxidation of benzyl alcohol at 380 ^{o}C for 1 h using O_2/hydroxyl = 0.6 and WHSV = 20 h^{-1}, and then were tested at 250 ^{o}C using O_2/hydroxyl = 0.6 and WHSV = 20 h^{-1}.

Table S1. The turnover frequency (TOF) of benzyl alcohol oxidation over various catalysts. [a]

Catalysts	V_{total} (cm³) [b]	D_{Au} (nm) [c]	$V_{Au-particle}$ (nm³) [d]	Amount of Au particles [d]	$S_{Au-particle}$ (nm²) [d]	S_{total} (cm²)	Surface Au Atoms [e]	Conv. (%) [f]	Converted Benzyl Alcohol [g]	TOF (h⁻¹)
NiO$_x$@Au/Ni-fiber	0.000609	25	4090	1.49×10^{14}	982	1462	1.86×10^{18}	95	3.18×10^{22}	17097
Au/SiO$_2$	0.000609	27	5153	1.18×10^{14}	1145	1351	1.72×10^{18}	6	0.2×10^{22}	1156
Au/Ni-fiber-W	0.000609	25	4090	1.49×10^{14}	982	1462	1.86×10^{18}	31	1.04×10^{22}	5591
NiO$_x$/Ni-fiber	---	---	---	---	---	---	---	6	---	
NiO$_x$@Au/Ni-fiber-W	0.000609	25	4090	1.49×10^{14}	982	1462	1.86×10^{18}	93	3.11×10^{22}	16720
Au/Ti-fiber	0.000609	30	7069	0.86×10^{14}	1414	1216	1.55×10^{18}	4	0.13×10^{22}	839
NiO$_x$/Ti-fiber	---	---	---	---	---	---	---	5	---	
NiO$_x$@Au/Ti-fiber	0.000609	27	5153	1.18×10^{14}	1145	1351	1.72×10^{18}	92	3.08×10^{22}	17907
Au/NiO-Ni-fiber	0.000609	24	3619	1.68×10^{14}	905	1522	1.94×10^{18}	30	1.00×10^{22}	5155
NiO$_x$@Au/NiO-Ni-fiber	0.000609	24	3619	1.68×10^{14}	905	1522	1.94×10^{18}	93	3.11×10^{22}	16031

[a] For all the catalysts, the gold loading is 4.0 wt%, and 0.3 g catalyst was used in testing experiments; [b] The total volume of gold ($V_{total} = 0.000609$ cm³) was calculated as: gold mass (0.3 g×0.04 = 0.012 g) was divided by the gold density (19.7 g/cm³); [c] The particle size was estimated from XRD patterns using Scherrer's equation; [d] The gold particles were assumed as hemisphere, and the volume of single gold particle is $\pi D_{Au}^{3}/12$, and the surface area is $\pi D_{Au}^{2}/2$; [e] The distance between the adjacent gold atoms is 0.28 nm, and one Au atom occupies the surface area of 0.0784 (0.28×0.28 = 0.0784) nm². [f] The weight hourly space velocity (WHSV) = 20 h⁻¹, and 6 g benzyl alcohol was fed into the reactor per hour; [g] Take the converted benzyl alcohol over the catalyst NiO$_x$@Au/Ni-fiber as example: the converted benzyl alcohol in one hour is 5.7 g (0.95×6 = 5.7 g), and the converted amount of benzyl alcohol molecule is 0.318×10^{23} (5.7 (g) / 108 (g/mol) = 0.0528 mol; 0.0528×6.02×10²³ = 0.318×10²³).

Table S2. The XPS results of several catalysts.

Catalyst	Compound type	B. E. (eV)	Peak Area	Fraction (%)
Sample 1	**O-1s**			
(working catalyst)	NiO	529.7	678	42
	Ni_2O_3	531.8	936	58
	Au-4f			
	Au^0	84.0	84	69
	Au^+	84.8	38	31
	Au^{3+}	86.2	0	0
	Ni-2p			
	NiO	854.4	2107	57
	Ni_2O_3	856.2	1665	43
Sample 2	**O-1s**			
(exhausted catalyst)	NiO	529.7	940	57
	Ni_2O_3	531.8	700	43
	Au-4f			
	Au^0	84.0	116	98.3
	Au^+	84.8	2	1.7
	Au^{3+}	86.3	0	0
	Ni-2p			
	NiO	854.4	2500	67
	Ni_2O_3	856.2	1260	33
Sample 3	**O-1s**			
(re-feeding O_2)	NiO	529.7	700	41
	Ni_2O_3	531.8	1000	59
	Au-4f			
	Au^0	84.0	83	67
	Au^+	84.8	40	33
	Au^{3+}	86.3	0	0
	Ni-2p			
	NiO	854.4	2170	58
	Ni_2O_3	856.2	1630	42

Reaction conditions: 250℃, O_2/hydroxyl = 0.6, WHSV = 20 h^{-1}. Pre-activation conditions: pre-activating the fresh samples at 380 ^oC for 1h in reaction steam of benzyl alcohol using O_2/hydroxyl = 0.6 and WHSV = 20 h^{-1}. **Sample 1**: the working NiO_x@Au/Ni-fiber; **Sample 2**: The sample 1 underwent the gas-phase reaction of benzyl alcohol with the absence of O_2 for 0.5h, and the obtained sample was called the exhausted catalyst; **Sample 3**: Sample 2 catalyzed benzyl alcohol oxidation by re-feeding O_2 again under the same conditions as for Sample 1.

Table S3 The conversion of benzyl alcohol over several catalysts.

Samples	O_2/ol	Conversion (%)	Selectivity (%)
Sample 1 (working catalyst)	0.6	95	99
Sample 2 (exhausted catalyst)	0	0.7	99
Sample 3 (re-feeding O_2)	0.6	92	99

Reaction conditions: 250ºC, O_2/hydroxyl = 0.6, WHSV = 20 h^{-1}. Pre-activation conditions: pre-activating the fresh samples at 380 ºC for 1h in reaction steam of benzyl alcohol using O_2/hydroxyl = 0.6 and WHSV = 20 h^{-1}. **Sample 1**: the working NiO$_x$@Au/Ni-fiber; **Sample 2**: The sample 1 underwent the gas-phase reaction of benzyl alcohol in the absence of O_2 for 0.5h, and the obtained sample was called the exhausted catalyst; **Sample 3**: Sample 2 catalyzed benzyl alcohol oxidation by re-feeding O_2 again under the same conditions as for Sample 1.

Table S4. The XPS results of the Au/Ni-fiber-W and Au/NiO-Ni-fiber catalysts.

Catalyst	Compound type	B. E. (eV)	Peak Area	Fraction (%)
Au/Ni-fiber-W	**O-1s**			
	NiO	529.7	696	63
	Ni_2O_3	531.8	370	37
	Au-4f			
	Au^0	84.0	101	88
	Au^+	84.7	14	12
	Au^{3+}	86.2	0	0
	Ni-2p			
	NiO	854.4	1576	73
	Ni_2O_3	856.2	601	27
Au/NiO-Ni-fiber	**O-1s**			
	NiO	529.7	1235	76
	Ni_2O_3	531.8	390	24
	Au-4f			
	Au^0	84.0	97	88
	Au^+	84.8	13	12
	Au^{3+}	86.3	0	0
	Ni-2p			
	NiO	854.4	2950	83
	Ni_2O_3	856.2	585	17

The Au/Ni-fiber-W and Au/NiO-Ni-fiber catalysts are the same samples as in Table 1 (Entries 2 & 8, respectively) in manuscript after calcination and reactivity test. Reaction conditions: 250ºC, O_2/hydroxyl = 0.6, WHSV = 20 h^{-1}. Pre-activation conditions: pre-activating the fresh samples at 380 ^{o}C for 1h in reaction steam of benzyl alcohol using O_2/hydroxyl = 0.6 and WHSV = 20 h^{-1}.

Supplementary Discussion 1: The formation of the Au@NiO ensembles

The sinter-locked Ni-microfiber was heated in air at 600 °C for 2 h prior to loading Au. The HAuCl$_4$-Ni galvanic exchange reaction almost didn't take place due to the formation of bulk NiO (Fig. SD1). Although there may be a reaction between HAuCl$_4$ and NiO (H$^+$ + NiO = Ni^{2+} + H$_2$O), the reaction is too trivial to be considered, which could be confirmed by the absence of NiCl$_2$ (XRD patterns not shown). Therefore, the active ensembles of the catalyst Au/NiO-Ni-fiber can be determined as Au@NiO.
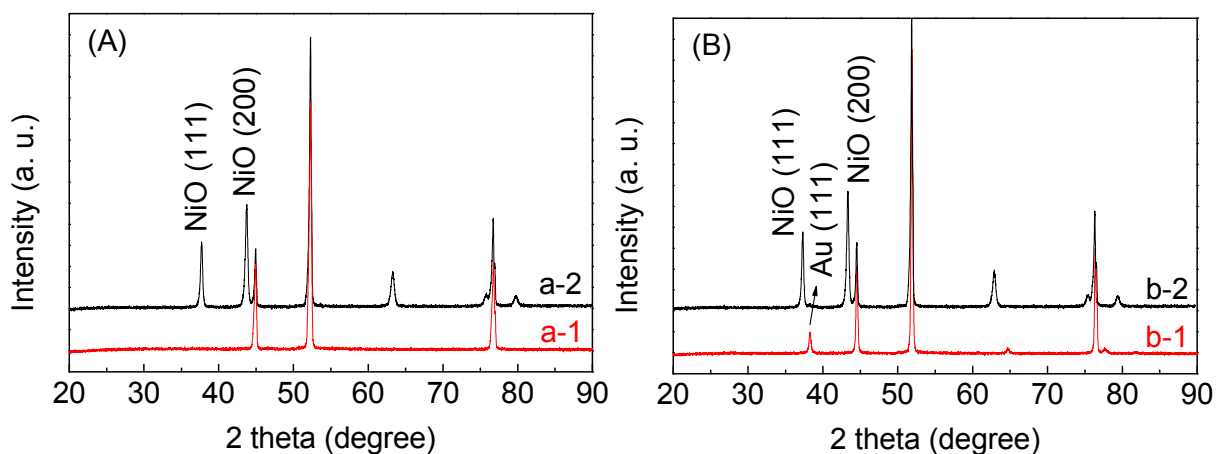
Fig. SD1. XRD patterns of the sinter-locked Ni-microfiber and the catalyst samples. (A) a-1: pure sinter-locked Ni-microfiber; a-2: pure sinter-locked Ni-microfiber treated in air at 600 °C for 2 h; (B) b-1: the as-prepared catalyst Au/Ni-fiber prepared on pure sinter-locked Ni-microfiber (same sample of a-1) just after galvanic reaction before drying and calcining; b-2: the as-prepared catalyst Au/NiO-Ni-fiber (gold loading of 4 wt%) prepared on the treated sinter-locked Ni-microfiber (same sample of a-2) just after galvanic reaction before drying and calcining.

Supplementary Discussion 2: The analysis of XPS data

For the working $NiO_x@Au/Ni$-fiber, the surface atom ratio of $O_{(531.8eV)}/Ni_{(856.2eV)}$ was quantitatively determined using the following calculations. Firstly, the Ni^{2+}/Ni^{3+} ratio can be obtained from the Ni 2p peak areas of NiO and Ni_2O_3, which are 2107 and 1665, respectively. The Ni^{2+}/Ni^{3+} ratio is 57:43 (2107:1665), and the O_{NiO}/O_{Ni2O3} ratio is 42:58 (678:936). The total surface atom ratio of Ni/O is 42:49.4, which was given by the XPS total scanning data. Therefore, the surface $O_{(531.8eV)}/Ni_{(856.2eV)}$ atom ratio is quantitatively determined to be 1.55 ($[0.58 \times 49.4]/[0.44 \times 42] = 1.55$).

For the same $NiO_x@Au/Ni$-fiber sample after experiencing gas-phase reaction of benzyl alcohol with the absence of O_2 for 0.5h, the surface $O_{(531.8eV)}/Ni_{(856.2eV)}$ atom ratio was quantitatively determined using the same calculation. The Ni^{2+}/Ni^{3+} ratio is 66:34, and the O_{NiO}/O_{Ni2O3} ratio is 57:43. The total surface atom ratio of Ni/O is 42:47. Therefore, the $O_{(531.8eV)}/Ni_{(856.2eV)}$ atom ratio is quantitatively determined to be 1.46 ($[0.43 \times 47]/[0.33 \times 42] = 1.46$), which coincided almost stoichiometrically ($100\% \times 1.46/1.5 = 97.3\%$).

The XPS peaks of NiO and Ni_2O_3 over the working catalyst $NiO_x@Au/Ni$-fiber is 2107 and 1665, respectively, and the whole area of Ni is 3772 ($2107 + 1665 = 3772$). The XPS peaks of NiO and Ni_2O_3 over the exhausted catalyst $NiO_x@Au/Ni$-fiber is 2500 and 1260, respectively, and the whole area of Ni is 3760 ($2500 + 1260 = 3760$). Compared the area of XPS peaks of NiO and Ni_2O_3 over the two samples, it is found that: (1) The whole area of Ni over the two catalysts remains unchanged (3772 v.s. 3760); (2) The peak area of Ni_2O_3 decreased by 405 from 1665 of the working catalyst to 1260 of the exhausted one; (3) The peak area of NiO increased by 393 from 2107 of the working catalyst to 2500 of the exhausted one; (4) The reduced area of Ni_2O_3 is almost equal to the increased area of NiO ($100\% \times 393/405 = 97\%$). Therefore, the above results showed that reduced Ni_2O_3 transformed to NiO.

Supplementary Discussion 3: The analysis of XAFS data

Because the support of the pre-activated catalyst $NiO_x@Au/Ni$-fiber is Ni-fiber, so that the Ni_2O_3/Ni^0 molar ratio is very low and the trend of changes of Ni_2O_3 content is difficult to be detected. To investigate the difference of the absorption intensity of NiO and Ni_2O_3, another two samples were prepared, including pure NiO and the pre-activated catalyst Au-5-NiO-4/Ti (Au loading of 5 wt%, and NiO loading of 4 wt%).

Clearly, the absorption intensity at 8350 eV of the pre-activated catalyst Au-5-NiO-4/Ti is higher than that of the pure NiO (Fig. SD2A). Additionally, the Ni-O coordination of the pre-activated catalyst is higher than that of the pure NiO (Fig. SD2B). The only difference of Ni state over the two samples is that the Ni_2O_3 content of the pre-activated catalyst Au-5-NiO-4/Ti is much higher than that of the pure NiO (detected by XPS, not shown). Therefore, the existence of Ni_2O_3 is favorable to increase the absorption intensity of whiteline.
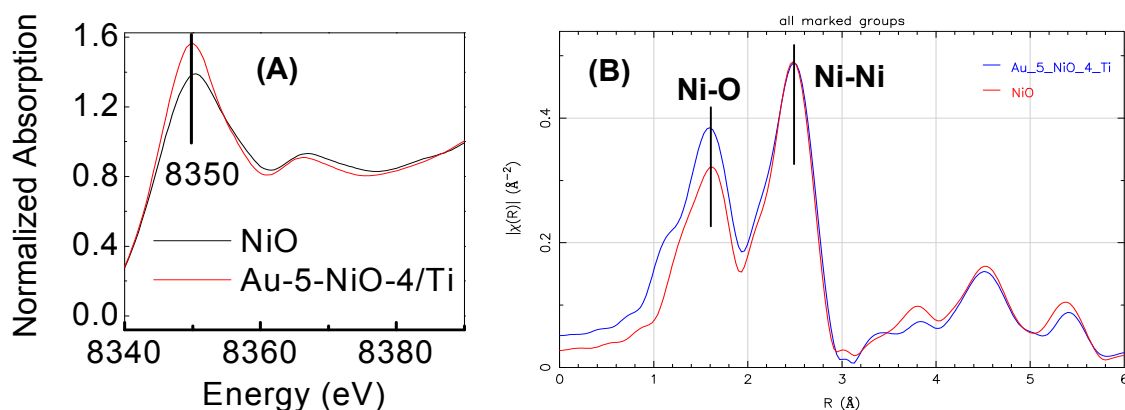
Fig. SD2. Ni K-edge XANES (A) and modulus of the Fourier-transform of Ni K-edge signal (B) over pure NiO and the pre-activated catalyst Au-5-NiO-4/Ti (Au loading of 5 wt%, and NiO loading of 4 wt%). Pre-activation conditions: same as in Fig. S1.

The absorption intensity at the energy of 8350 eV of the exhausted catalyst is slightly lower than the

working one, and subsequently increased to the previous level by re-feeding O_2 into the reaction stream.

Combining the XPS results, it could be inferred that the high-low-high change of the absorption intensity at

8350 eV is caused by the high-low-high change of Ni_2O_3 content.

References

[S1] D. K. Harris, D. R. Cahela and B. J. Tatarchuk, *Compos. A: Appl. Sci. Manuf.*, 2001, **32**, 1117.

[S2] Y. Lu, H. Wang, Y. Liu, Q. S. Xue, L. Chen and M.Y. He, *Lab Chip*, 2007, **7**, 133.

[S3] F. T. Jiang, Y. Z. Fang, Y. Liu, L. Chen, Q. S. Xue, Y. Lu, J. X. Lu and M. Y. He, *J. Mater. Chem.*, 2009, **19**, 3632.

[S4] Y. Liu, H. Wang, J. F. Li, Y. Lu, H. H. Wu, Q. S. Xue and L. Chen, *Appl. Catal. A*, 2007, **328**, 77.

[S5] M. M. Deng, G. F. Zhao, Q. S. Xue, L. Chen and Y. Lu, *Appl. Catal. B*, 2010, **99**, 222.

[S6] G. F. Zhao, H. Y. Hu, M. M. Deng and Y. Lu, *Chem. Commun.*, 2011, **47,** 9642.

[S7] B. Lengeler and P. Eisenberger, *Phys. Rev. B*, 1980, **21**, 4507.

[S8] J. P. Mao, M. M. Deng, L. Chen, Y. Liu and Y. Lu, *AIChE J.*, 2010, **56**, 1545.